

# DEVELOPMENT OF A TOWED UNDERWATER LAUNCH PLATFORM

K. N. Parthasarathy \*  
B. E. McGrath \*  
D. A. Frostbutter \*  
J. J. Wozniak

The Johns Hopkins University  
Applied Physics Laboratory  
Laurel, Maryland

19961213064

## Abstract

The concept of a new test facility to evaluate the underwater launch and flight performance of full-scale missiles and associated launcher systems is described. Results from preliminary studies on estimates of the platform dimensions, hydrodynamic characteristics, and platform response to a missile launch impulse are included. The VSAERO panel method code was used to generate hydrodynamic force and moment coefficients for the condition of steady tow at 5 knots. These coefficients were then used to evaluate the platform trim stability under steady tow conditions. Calculations indicate that the platform is stable during all three phases of operation: missile in tube, empty tube, and tube fully flooded. Preliminary estimates of the platform response due to a launch impulse show a recoil that is not expected to significantly alter the fidelity of the in-tube trajectory data.

## 1.0 Introduction

Since the 1950s, the U.S. Navy has successfully developed a number of strategic and tactical missile weapon systems that are launched vertically from submerged, forward-moving submarines. These weapon systems cover a wide spectrum of designs. These designs range from the Trident II intercontinental ballistic missile to the Tomahawk Vertical Launch System (VLS). The Trident II missile is nearly 7 feet in diameter, weighs over 100,000 pounds, and is launched from a submarine moving at near-zero forward speed, while the Tomahawk VLS, which is 21 inches in diameter in torpedo tube, weighs less than 4000 pounds and is capable of being launched at moderate forward-way with maneuvering.

The successful development of these complex weapon systems is in no small measure a result of the ability to test, evaluate, and understand the physics of underwater launch. Historically, the engineering development of a new submarine-launched missile combines both computer simulation and subscale or full-scale test with approximation to the actual launch conditions. While some launch phenomena can be mimicked in this manner, complex interactions between the missile, launcher, and the environment can be missed. Extremely costly "fixes" and programmatic delays can arise if complete weapon system testing is delayed until deployed on the actual submarine. The need for high-fidelity and robust testing during the developmental phase of a missile is important; however, this need is tempered with the constraint to control costs associated with developing and maintaining a full-scale launch test facility.

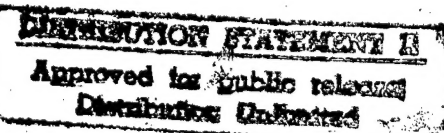
One potential solution to this ever-present engineering dilemma is a concept called the Towed Underwater Launch Platform (TULP). The TULP is a submersible, towed platform that simultaneously replicates the hydrostatic pressure (depth) and the submarine deck flow field (crossflow velocity) at full scale to capture the complex phenomenology of underwater launch. Sufficient flexibility is built into the design to accommodate a diverse range of missile types and test requirements.

## 2.0 TULP Concept Description

The overall guidance in developing the TULP concept was finding a low-cost, full-scale facility for missiles and launchers undergoing engineering development. References 1-3 document the initial study results that defined the TULP concept and explored a point design from the perspective of physical features (weight, moments of inertia, displacement, and reserve buoyancy), hydrodynamic characteristics (drag, tow horsepower

\* Senior Member, AIAA

Copyright © American Institute of Aeronautics and Astronautics, Inc., 1996, All rights reserved.



requirement, impulse response, etc.), a preliminary depth control/deballasting system, and an operational scenario.

The TULP configuration is shown in Figures 1 and 2. The principal TULP components consist of a support frame with deck plating, a launch tube housed within an outer streamlined structure, a multiple pontoon buoyancy system, and a closed-loop hovering/deballasting system. In addition, four free-flooding tubular supports between the deck frame and the mount tube are shown to provide lateral and torsional mount tube rigidity. The rectangular form of the deck has high hydrodynamic inertia (added mass) in the vertical plane to minimize platform recoil to the launch pulse. The structure was sized to control platform recoil from the launch pulse with limitation to allow the system to operate from existing Navy wharf facilities.

TULP buoyancy is provided by a hard-tank pontoon system secured to the platform deck and by the faired compartment surrounding the launch tube. The two large pontoons, outboard of the launch tube, serve as seawater blow/flood tanks and as a compartment to house valves and pressure sensors associated with the closed-loop depth-control/deballasting system.

The free-flooding structure ("fairwater") added to the main deck replicates the flow over the submarine near the launch tube region. The fairwater deck is shown asymmetric about the platform centerline. To help reduce any yaw motion that would be induced by dynamic pressure asymmetry during tow operations, a flow-through path is shown.

The structure encircling the launch tube provides a watertight compartment to house the launch tube, gas generator, and test instrumentation. The compartment allows access to launch equipment during surface operations. A free-flooding fairing is added to the encircling structure to minimize drag for reduced tow power during crossflow tests. Access to the housing is provided through a service hatch located under the fairwater deck. The lower portion of the faired structure contains lead ballast to aid in platform stability. Forward-way is provided by means of a support Navy tugship that is outfitted with launcher and fire control subsystems. A tow cable with strength member, electrical power, and communication line would provide a safe standoff distance between the TULP and towship. In keeping with past safe practice, an inert launch test vehicle (LTV) would be the test missile employed for engineering development of any new system.

Table 1 is a compilation of the results of a recent TULP sizing study. Preliminary estimates of the TULP component structure were generated using standard marine design practices for calm-to-moderate sea conditions (it is assumed that engineering testing would not be performed under high sea-state conditions). The pontoon size and lead ballast were selected to maintain a positive submerged metacentric height under the following conditions:

Table 1. Estimated principal characteristics of Towed Underwater Launch Platform.

Principal Dimensions	
Overall length, ft	60.0
Overall beam, ft	40.0
Overall height, ft	47.5
Surfaced draft, ft	39.5
Physical Characteristics	
Weight (excluding test vehicle), lb	360,000
Submerged displacement (excluding free flooding), lb	490,000
Reserve buoyancy, lb	24,000
Roll and pitch moment of inertia, slug-ft <sup>2</sup>	$3.0 \times 10^6$
Center of gravity (C.G.),* ft	-8.8
Hydrodynamic Characteristics	
Center of buoyancy (C.B.),* ft	-4.2
Submerged metacentric height (C.B. - C.G.), ft	4.6
Forward-way drag @ 5 knots, lb	$\sim 6,500$
Submerged tow @ 5 knots, hp	$\sim 100$
Heave added mass (including free flooding), slugs	$1.65 \times 10^6$
Roll and pitch added moment of inertia, slug-ft <sup>2</sup>	$6.25 \times 10^6$
Roll and pitch natural period, s	18 to 19
Depth Control/Deballasting System	
Ballast tank volume (each), ft <sup>3</sup>	850
Ballast tank capacity (each), lb	55,000
Maximum flow rate @ DP = 50 PSID, lb/s	540

\*The vertical positions of C.G. and C.B. are defined with reference to the axis system shown in Figure 1. C.G. is with test vehicle in tube.

a missile in the launch tube, an empty launch tube, and a launch tube filled with seawater.

### 3.0 Hydrodynamic Analysis

#### 3.1 VSAERO Panel Code

This paper addresses the hydrodynamic and stability issues associated with steady-state tow. In order to assess the stability characteristics of the TULP in steady tow, a hydrodynamic analysis was performed using a low-order panel method code, VSAERO.<sup>4,5</sup> The code calculates the inviscid, linearized potential flow external to a body. An integral boundary-layer method may be coupled with VSAERO to obtain an estimate of the viscous effects. For incompressible and irrotational flow, the potential flow will satisfy Laplace's equation. The potential flow must also satisfy the integral equations obtained from the application of Green's theorem. VSAERO solves for the flow potential by solving the integral equation from Green's theorem on the surface boundary using a constant strength

distribution of sources and doublets along a defined set of body panels. The panel method solution is obtained by solving the integral equation as a set of equations and unknowns equal to the number of panels defining the body surface. For the solution of the TULP configuration, initially a zero normal velocity boundary condition was applied on each body panel.

The vorticity shed by the body into the flow is modeled by a wake off the trailing edge of the body. The wake is also modeled by a set of panels, by defining wake grid planes and wake lines. The wake is allowed to relax or conform to a steady-state shape that satisfies the normal velocity boundary condition across the wake panels. The integral boundary-layer method can compute laminar and turbulent attached flow, boundary-layer transition and separation points, and relaminarization. Application of the integral boundary-layer method adds a transpiration term in the boundary condition to account for the boundary-layer displacement thickness. The data were postprocessed with the OMNI3D code,<sup>6</sup> and wake preprocessing was performed using the SPIN code.<sup>7</sup>

The analysis was performed using the computer facilities at the U.S. Navy Hydrodynamic/Hydroacoustic Technology Center at the Naval Surface Warfare Center, Carderock Division, Bethesda, Maryland. The calculations were performed on a Silicon Graphics Power Challenger with six 75-MHz processors and 2048 Mbytes of memory.

The hydrodynamic coefficients computed by the VSAERO code were used to evaluate the stability of the platform in steady tow. The following section describes the approach used to develop the fully submerged platform trim stability under steady tow.

### 3.2 Trim Equations for the TULP vehicle

Reference 8 contains the equations of motion for a submarine. For the TULP trim analysis, the components for towcable tension and towpoint location were added. Also, the force and moment coefficient definitions were replaced with the nomenclature consistent with VSAERO nomenclature. In addition, the following assumptions were made: steady horizontal flight, all coupled hydrodynamic terms set to zero, all acceleration and rotational rates nulled, and zero sideslip and roll angles. With these assumptions, the following set of equations result for the axial and normal force and the pitching moment:

Axial force equation

$$\frac{1}{2} \rho u^2 A C_A + (W - B) \alpha - T_x = 0 \quad (1)$$

Normal force equation

$$\frac{1}{2} \rho u^2 A (C_N + C_{N\alpha} \alpha) - (W - B) - T_z = 0 \quad (2)$$

Pitching moment equation

$$\begin{aligned} \frac{1}{2} \rho u^2 A (C_m + C_{m\alpha} \alpha) + (x_G W - x_B B) \\ - (z_G W - z_B B) \alpha + T_x z_{TP} - T_z x_{TP} = 0 \end{aligned} \quad (3)$$

Equations 1, 2, and 3 are solved simultaneously to obtain the equation for  $\alpha_{\text{trim}}$ :

$$\begin{aligned} \alpha_{\text{trim}} = \\ \frac{1}{2} \rho u^2 A (C_m l - C_{A\alpha} z_{TP} + C_{N\alpha} x_{TP}) - (x_G W - x_B B) + x_{TP} (W - B) \\ - \frac{1}{2} \rho u^2 A (C_{m\alpha} l - C_{N\alpha} x_{TP}) + (z_G W - z_B B) - z_{TP} (W - B) \end{aligned}$$

where

$$\begin{aligned} B &= \text{buoyancy, lbf} \\ W &= \text{weight, in air, lbf} \\ u &= \text{component of velocity along body } x \text{ axis} \\ T_x, T_z &= \text{towcable tension along body } x \text{ and } z \text{ axis} \\ \text{systems} & \\ C_A &= \text{axial force coefficient at } \alpha = 0 \\ C_N &= \text{normal force coefficient at } \alpha = 0 \\ C_m &= \text{pitching moment coefficient at } \alpha = 0 \\ C_{N\alpha} &= \text{slope of the normal force coefficient at } \alpha = 0 \\ C_{m\alpha} &= \text{slope of the pitching moment coefficient at} \\ &\alpha = 0 \\ x_B, z_B &= x \text{ and } z \text{ coordinates of center of buoyancy} \\ &(\text{C.B.}), \text{ft} \\ x_G, z_G &= x \text{ and } z \text{ coordinates of center of gravity (C.G.), ft} \\ x_{TP}, z_{TP} &= x \text{ and } z \text{ coordinates of the towpoint attachment, ft} \\ \alpha &= \text{angle of attack, deg} \\ \alpha_{\text{trim}} &= \text{trim angle of attack, deg} \\ \rho &= \text{density of seawater, } 1.9905 \text{ slug/ft}^3 \\ A &= \text{reference area (86.59 ft}^2\text{)} \\ l &= \text{reference length (10.5 ft)} \end{aligned}$$

### 4.0 Results and Discussion

For the initial VSAERO calculations, the TULP geometry was modeled with a bluff base. The launch tube fairing consisted of a symmetric airfoil. The approach flow velocity was 5 knots (8.44 ft/s) and the Reynolds number ( $R_e$ ) was 7 million based on a reference length of 10.5 ft (launch tube diameter). The flow angularity was 0°. Figure 3 shows an isometric rear view of the bluff base configuration. Imposed on the configuration surface are the surface pressure coefficient distribution ( $C_p$ ), the surface streamlines, and VSAERO geometry panels. The dark shaded regions represent high- and low-pressure regions. The wake shedding off the bluff base is represented by the panels shown to the left of and aft of the body. The surface streamlines are shown as streaks along the surface of the body. The surface streamlines terminate at locations where VSAERO determined the boundary-layer

shape factor to be of a value that indicates flow separation. Therefore, the regions where the surface streamlines have terminated approximately coincide with regions of flow separation. The initial bluff base calculations revealed flow separation along the launch tube fairing trailing edge, fairwater deck trailing edge, and sharp leading edge of the bow. The calculations also revealed a large unsteady and turbulent wake shedding off the bluff base.

The TULP geometry was modified to alleviate some of the flow problems. The stern of the main deck was lengthened by 6 ft, the overall structure was streamlined (ogive shape) over the aft 22 ft of the main deck, and the bow was rounded along the leading edge. Additional streamlining of the launch tube was not performed at this time. The modified TULP geometry and VSAERO paneling are shown in Figure 4. VSAERO calculations were then performed with the modified geometry. The modified TULP configuration consisted of approximately 3500 body panels and 770 wake panels. The solutions were obtained by using a 14-block formulation for the Gauss-Seidel iterative solver. The solutions were coupled with an integral boundary-layer method to obtain 163 surface streamlines and boundary-layer calculations. Each complete VSAERO calculation included 6 wake iterations or relaxations and 20 inviscid/viscous iterations. The CPU time for each solution ranged between 510 and 525 s.

A matrix of flow conditions for a steady tow speed of 5 knots for the modified TULP was defined and the computations were performed. The matrix is for angles of attack ( $\alpha$ ) of  $0.0^\circ, \pm 1.0^\circ, \pm 2.5^\circ$ , and  $\pm 5.0^\circ$  each at angles of sideslip ( $\beta$ ) of  $0.0^\circ, \pm 1.0^\circ, \pm 2.5^\circ$ , and  $\pm 5.0^\circ$ . Table 2 lists the axial ( $C_A$ ), normal ( $C_N$ ), and side ( $C_Y$ ) force coefficients as well as the pitching moment ( $C_m$ ), rolling moment ( $C_I$ ), and yawing moment ( $C_n$ ) coefficients. The non-zero sideslip angle computations are not presented in this paper.

Figure 5 shows results from VSAERO at an angle of attack of  $+5^\circ$  for the modified TULP configuration. The figure shows the surface streamlines and wake. Comparison of the wake of the modified TULP configuration (Figure 5) and the bluff body TULP configuration (Figure 3)

shows that the wake off the streamlined TULP is not as unsteady and turbulent as the wake off the bluff base TULP. The streamlining of the stern did not appear to eliminate flow separation along the trailing edge. However, additional streamlining may help reduce or eliminate this region of flow separation. Flow separation along the bow leading edge appeared to be eliminated. Additional streamlining is recommended to optimize the TULP configuration for reducing flow separation, reducing drag, and further reducing the turbulent wake. This additional design work was beyond the scope of this study.

Figures 6 through 9 depict the evolution of the hydrodynamic forces ( $C_A, C_N, C_Y$ ) and pitching moment ( $C_m$ ) as a function of the number of VSAERO iterations for the zero angle of attack and zero angle of sideslip case. In each figure, the first seven data points are the inviscid calculations that include one rigid wake and six wake relaxations. The next 19 data points are the remaining inviscid/viscous calculations. These remaining iterations are where VSAERO couples the integral boundary-layer method with the inviscid calculations. Oscillations in the coefficients for the viscous calculations are due to the application of the transpiration term in the solution. The transpiration term is applied in the boundary condition to account for the boundary-layer displacement thickness. The amount of transpiration is adjusted on each iteration and causes small differences in the pressure distribution from iteration to iteration. These differences in the pressure distribution show up in the integrated hydrodynamic forces and pitching moment. These oscillations are purely numerical in nature and are not an expected physical phenomenon. In all cases, the final coefficient value is taken at the last inviscid/viscous iteration.

Figure 6 shows the axial force coefficient ( $C_A$ ) as a function of iteration number. The viscous iterations show a large increase in  $C_A$  due to addition of the skin friction and transpiration effects. The normal force coefficient ( $C_N$ ) (see Figure 7) and the side force coefficient ( $C_Y$ ) (see Figure 8) have a near-constant inviscid value. The viscous iterations show a small decrease in the magnitude of the normal force coefficient and a small increase in the

Table 2. Hydrodynamic force and moment coefficients.

$\alpha$ (deg)	$C_A$	$C_N$	$C_m$	$C_Y$	$C_I$	$C_n$
-5.0	0.3136	-1.2040	-7.0830	0.0692	0.2568	-0.3968
-2.5	0.4105	0.0515	-4.3570	0.0376	0.2457	-0.1623
-1.0	0.4586	0.6288	-2.3330	0.0298	0.3268	-0.0383
0.0	0.4768	1.0170	-1.0060	0.0430	0.3430	0.0467
1.0	0.4966	1.5180	0.1640	0.0320	0.2757	0.1386
2.5	0.4897	2.0020	2.3640	0.0197	0.3833	0.2741
5.0	0.4817	2.9050	5.8400	0.0088	0.2787	0.5270

Length = 66 ft; launch tube diameter = 10.5 ft; velocity = 5 knots = 8.44 ft/s; Reynolds number ( $R_e$ ) = 7 million;  $C_{bar} = 10.5$  ft;  $S_{ref} = 86.59$  ft<sup>2</sup>;  $S_{span} = 10.5$  ft;  $\alpha = \pm 5.0^\circ$ ;  $\beta = 0^\circ$ .

magnitude of the side force coefficient. The small increase in side force may be due to an effective increase in asymmetry due to the displacement thickness. The pitching moment coefficient ( $C_m$ ) variation with iteration number is illustrated in Figure 9. The moment reference center for these calculations was chosen to be along the lower surface of the main deck, near the juncture point of the centerline of the launch tube and the lower surface of the main deck. The inviscid iterations show a nearly constant negative value of the pitching moment coefficient. The viscous iterations show a less negative (decrease in magnitude) pitching moment coefficient due to a smaller viscous normal force coefficient.

Figures 10 through 12 show the variation of the hydrodynamic forces as a function of angle of attack. Each figure shows the VSAERO results at zero angle of sideslip and a Reynolds number of 7 million.  $C_A$  increases with angle of attack up to  $1^\circ$  and then decreases with a further increase in angle of attack (Figure 10).  $C_N$  increases nearly linearly between  $\pm 5^\circ$  angle of attack (Figure 11). There appear to be very small nonlinear effects in the normal force coefficient. The asymmetric shape, which is due to the combination of the fairwater and main decks, is most likely the cause for the small nonlinear effects as a function of angle of attack. The magnitude of the side force coefficient ( $C_Y$ ) is non-zero because of the asymmetric shape of the TULP configuration (Figure 12).  $C_Y$  decreases in magnitude with increasing angle of attack because the geometry is asymmetric about the  $x$ - $z$  plane. The asymmetry is due to the lateral offset of the fairwater deck. At negative angles of attack, the asymmetry is fully exposed to the onset flow, resulting in a larger asymmetric side force. However, at positive angles of attack, the asymmetry is partially shielded from the onset flow, resulting in a smaller asymmetric side force.

The variation of the hydrodynamic moments with angle of attack is portrayed in Figures 13–15. Once again, the VSAERO results are for zero angle of sideslip and a Reynolds number of 7 million. Figure 13 shows that  $C_m$  increases linearly between  $\pm 5^\circ$  angle of attack. There are small nonlinear effects near  $\pm 5^\circ$  angle of attack. The nonlinear effects arise from the nonlinear effects of normal force, which is likely due to the asymmetric shape of the modified TULP configuration. The positive slope of the pitching moment suggests an unstable configuration. However, when buoyancy, weight, and tow forces are considered, the TULP is stable, as shown in a later section of this paper. The rolling moment coefficient ( $C_l$ ) is non-zero at all angles of attack and varies between 0.25 and 0.39 (Figure 14).  $C_l$  is non-zero because of the geometric asymmetry about the  $x$ - $z$  plane. The yawing moment coefficient ( $C_n$ ) increases linearly between  $\pm 5^\circ$  angle of attack (Figure 15).

The VSAERO computed coefficients were used in

conjunction with mass, buoyancy, and towpoint estimates to compute the trim angle of attack ( $\alpha_{trim}$ ) for the refined TULP configuration, under steady-state tow. The trim angle of attack was computed for three different states during the underwater launch sequence of a Trident-size Launch Test Vehicle (LTV). The three states are LTV in launch tube (prior to launch), launch tube empty (just after launch), and the launch tube flooded with seawater (after launch). The empty launch tube represents the “worst case” in terms of platform stability due to the reduced submerged metacentric height (i.e., the distance between the center of gravity and the center of buoyancy). Under all three conditions, the calculations show that the modified TULP configuration under steady tow will trim at an angle of attack less than or about  $1.0^\circ$  (Table 3).

Table 3. Platform stability under steady tow.

Launch State	Submerged Metacentric Height (ft)	Trim Angle of Attack (deg)
LTV in launch tube	4.6	1.03
Launch tube empty	1.3	0.66
Launch tube flooded	4.3	0.97

The stability of the modified TULP is due to the placement of the buoyancy pontoons along the deck and the lead ballast at the bottom of the launch tube. While this study shows stable steady-state tow performance with small angles of attack, a more comprehensive dynamic model would need to be developed to explore the full range of platform tow motions.

Another important aspect of the TULP concept is its time history response to an LTV test launch. Launching an LTV or missile involves a gas or steam generator with an impulse load transmitted to the launching platform. The platform response must be sufficiently small to ensure that the platform recoil does not alter the trajectory of the LTV or corrupt the collection of vital engineering data. The recoil of the platform is a function of the launch impulse as well as the mass and added mass of the platform. The TULP has a large hydrodynamic added mass in heave due to the shape and size of the main deck.

In the concept study of Ref. 1, a transfer function approach was used to estimate the platform recoil during a launch of a Trident-size LTV. The analysis showed that the platform would initially recoil downward approximately 0.65 ft with a vertical velocity of about 1.4 ft/s. In comparison, the LTV will have traveled an in-tube distance of 40 ft and will have attained a velocity of nearly 60 ft/s. The response of a Trident submarine to a launch will be a small fraction of that of the test platform.

However, the difference in their respective response characteristics should not be significant in terms of assessing the in-tube and underwater flight performance of the LTV.

Subsequent to the initial launch impulse, the platform will experience a light condition (launch tube empty) followed by a gradual return to a constant weight trim as seawater floods the launch tube. A detailed transient analysis with a 6 degree-of-freedom simulation would be necessary to fully understand all of the response characteristics to a launch impulse. The USAERO code,<sup>9</sup> a time-dependent panel method code, can be used to evaluate the TULP response to a launch impulse. USAERO solves for the inviscid potential flow for single or multiple bodies in general motion. The USAERO code is a sister code to the VSAERO code and was initially developed from an early version of VSAERO. The VSAERO geometric inputs are the same as the geometric inputs required for USAERO.

### 5.0 Conclusions

A point design for a TULP is reported in this paper. The TULP concept has been configured to provide a test bed that replicates the hydrostatic pressure (depth) and the submarine deck flowfield (crossflow) at full scale to capture the complex phenomenology of underwater launch. The configuration provides a large submerged metacentric height for pitch and roll stability, is streamlined in the fore-aft direction for low forward-way drag, and has a high added mass in heave to control launch recoil motions.

VSAERO panel code calculations were performed on the initial TULP concept geometry to assess flow stability and hydrodynamic performance. These calculations revealed regions of flow instability and separation. The TULP geometry was revised to correct the flow problems, and then the complete hydrodynamic forces and moment coefficients were computed. The hydrodynamic coefficients were combined with information about mass, buoyancy, and towpoint location to show a small trim angle of attack under a variety of launch tube conditions. These results are encouraging indicators that the TULP concept could provide a viable test platform.

### 6.0 Recommendations for Future Work

The recoil of the platform to a launch impulse can be addressed with the USAERO code, an unsteady panel method code. USAERO uses the same geometry inputs as the VSAERO code and is a natural follow-on to the VSAERO results reported here. This paper only addressed the hydrodynamic stability of the platform in the pitch

plane. It is recommended that additional work be performed to address the tow stability with non-zero angles of sideslip. Also, a 6 degree-of-freedom simulation that includes the tow-cable dynamics should be performed. Model-scale tests of the TULP in a tow tank should be carried out to measure the forces and moments acting on the platform.

### 7.0 Acknowledgments

The authors wish to thank the Hydrodynamic/Hydro-acoustic Technology Center (H/HTC) at the Naval Surface Warfare Center, Carderock Division for use of the Center's computational resources, namely, the VSAERO code and computer time, for this study. The authors also thank Mr. James Fraser from Analytical Methods, Inc., for his help and guidance in using the VSAERO code. This study was funded by the U.S. Navy Strategic Systems Programs Office, and their help is also gratefully acknowledged.

### References

1. Wozniak, J. J., "A Study of Alternative Support Platforms for D5 Test Vehicle Underwater Launch Testing," JHU/APL Memorandum PM-7953, 5 June 1978.
2. Wozniak, J. J., "Follow-on Study of the Towed Underwater Launch Platform (TULP) Concept for Trident II Launch Test Vehicle (LTV) Testing," JHU/APL Memorandum PM-8342, 10 Oct 1978.
3. Konodi, M. A., "Preliminary Analysis of a Depth Control System for the Towed Underwater Launch Platform Concept for D5 Testing," JHU/APL Memorandum PM-8367, 12 Oct 1978.
4. Maskew, B., "Program VSAERO Theory Document, A Computer Program for Calculating Nonlinear Aerodynamic Characteristics of Arbitrary Configurations," NASA Contractor Report 4023, Sept 1987.
5. "VSAERO, A Computer Program for Calculating Nonlinear Aerodynamic Characteristics of Arbitrary Configurations: Users' Manual, Revision E.5," Analytical Methods Report, April 1994.
6. "OMNI3D, A Post-processor for VSAERO and USAERO: Version 3.251," Analytical Methods Report.
7. "SPIN, A Wake and Basic Data Preprocessor for VSAERO: User's Guide, Version 2.2," Analytical Methods Report.
8. Gertler, M., and Hagen, G. R., "Trim Equations for a Towed Vehicle," NSRDC Report 2510, June 1967.
9. "USAERO, A Time-Stepping Analysis for the Flow about Multiple Bodies in General Motion: Users' Manual, Revision C.4," Analytical Methods Report, Sept 1993.

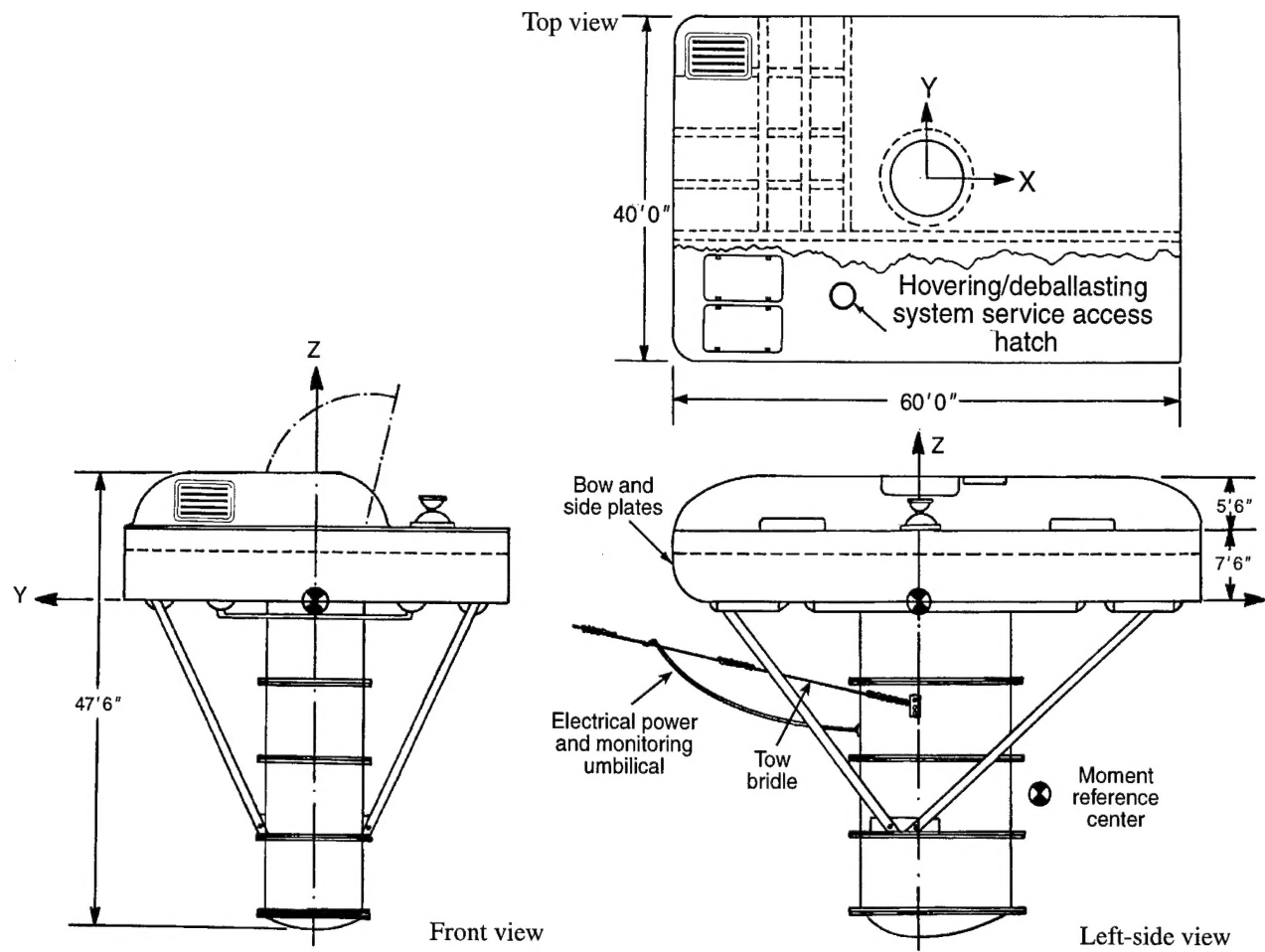


Figure 1. TULP configuration (three-view drawing).

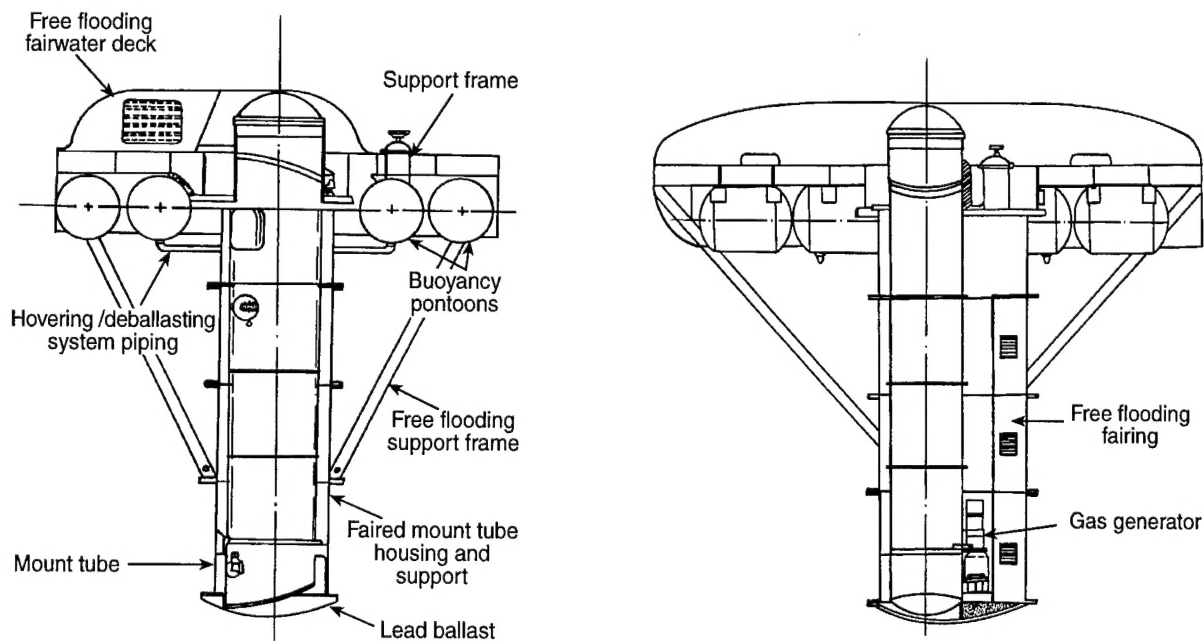


Figure 2. TULP configuration (cutaway views).

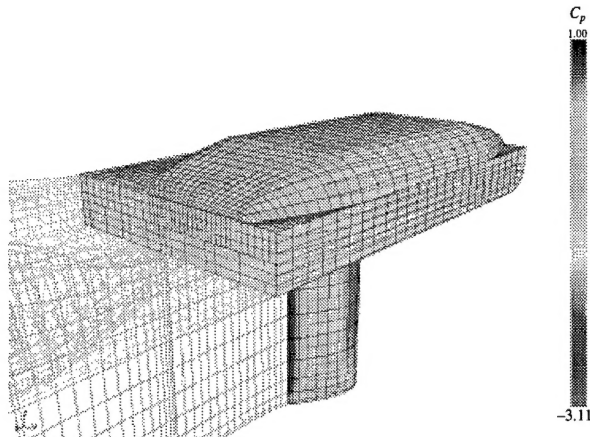


Figure 3. Launch platform (before geometry modifications).

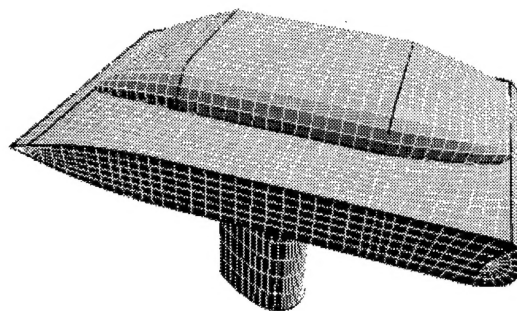


Figure 4. Modified TULP.

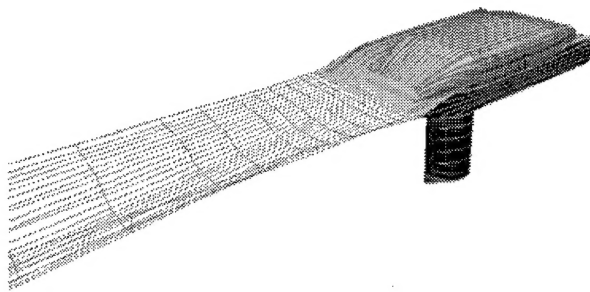


Figure 5. Boundary layer and wake flow for the modified TULP.

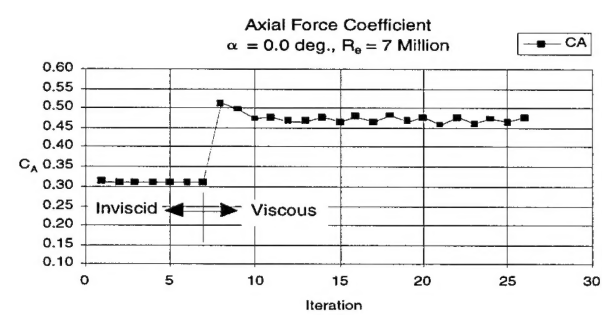


Figure 6. Axial force coefficient as a function of iteration number.

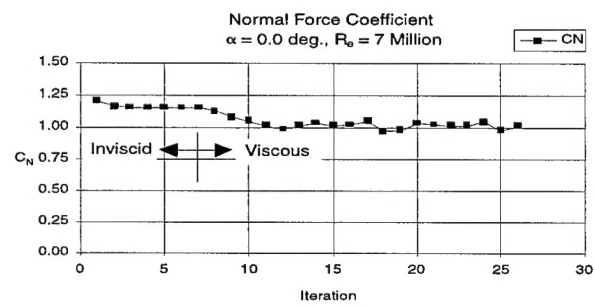


Figure 7. Normal force coefficient as a function of iteration number.

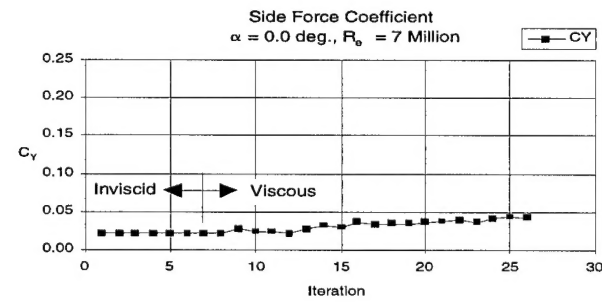


Figure 8. Side force coefficient as a function of iteration number.

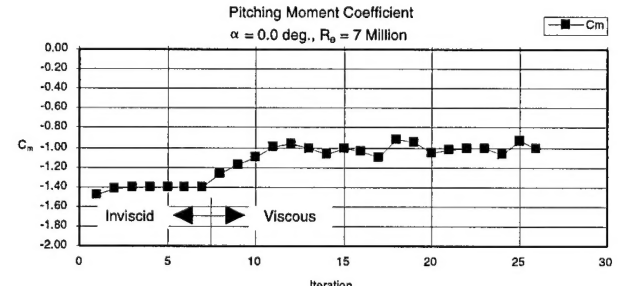


Figure 9. Pitching moment coefficient as a function of iteration number.

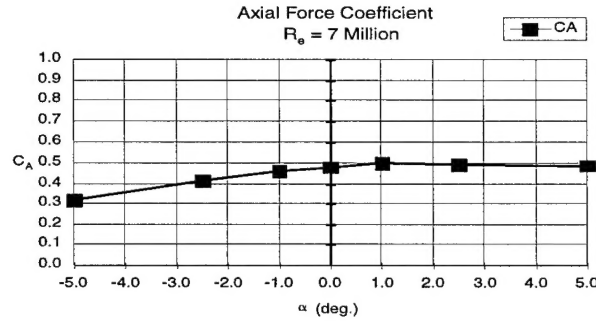


Figure 10. Axial force coefficient as a function of  $\alpha$ .

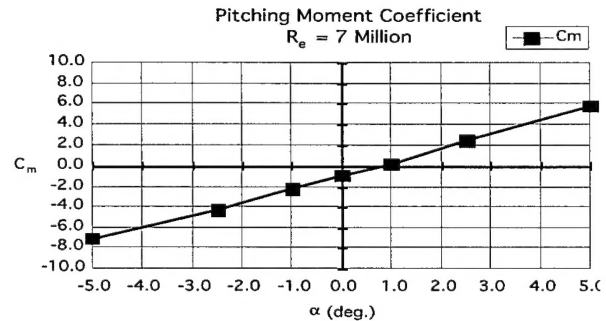


Figure 13. Pitching moment coefficient as a function of  $\alpha$ .

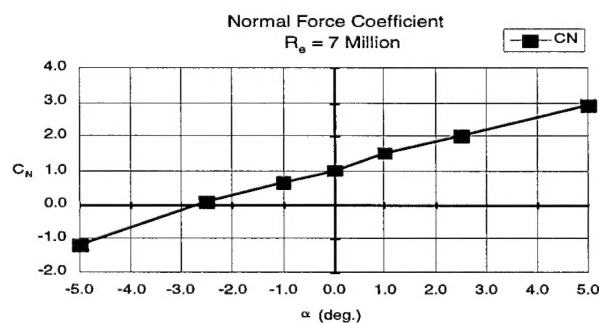


Figure 11. Normal force coefficient as a function of  $\alpha$ .

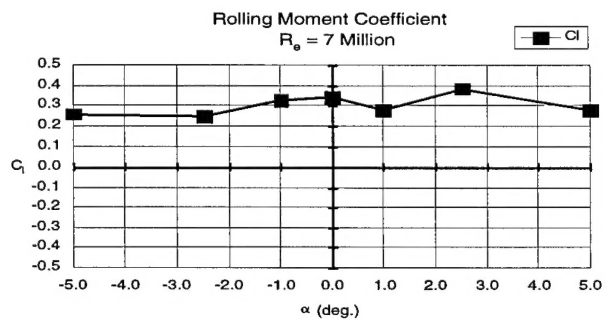


Figure 14. Rolling moment coefficient as a function of  $\alpha$ .

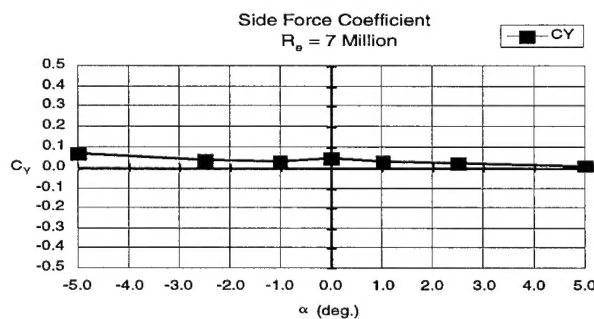


Figure 12. Side force coefficient as a function of  $\alpha$ .

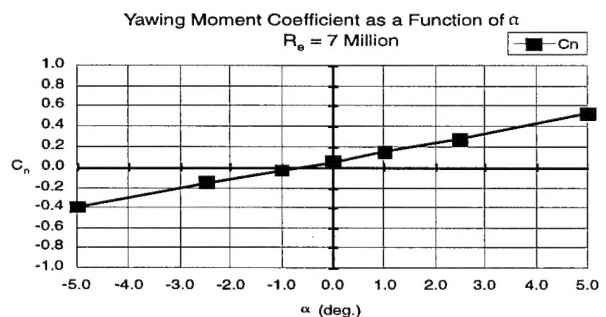


Figure 15. Yawing moment coefficient as a function of  $\alpha$ .



DEPARTMENT OF THE NAVY  
STRATEGIC SYSTEMS PROGRAMS  
1931 JEFFERSON DAVIS HWY  
ARLINGTON, VA 22241-5362

IN REPLY REFER TO

5531  
SP1622  
Ser U091896027

9 3 SEP 1996

From: Director, Strategic Systems Programs  
To: Director, The Johns Hopkins University  
Applied Physics Laboratory  
(Attn: L. Croston)  
Johns Hopkins Road  
Laurel, MD 20723-6099

Subj: CLEARANCE OF MATERIAL FOR PUBLIC RELEASE; SSP SECURITY  
REVIEW CASE 96-55

Ref: (a) JHU/APL ltr 96-173 of 29 Aug 96

Encl: (1) Paper, "Development of a Towed Underwater Launch  
Platform"

1. Enclosure (1), forwarded by reference (a), has been reviewed  
and is approved for **unlimited distribution**.

*P. M. Wallace*

P. M. WALLACE  
By direction

Copy to: (w/o encl)  
LMMS, Sunnyvale, (T. Tucci)

xc: / K. Parthasarathy  
L. Levy  
J. Gibson

UNCLASSIFIED  
091896027/000



STRATEGIC SYSTEMS PROGRAMS  
WASHINGTON, DC 20376-5002